Nonlinear Set-based Model Predictive Control for Exploration: Application to Environmental Missions

A. Anderson [*,**] **J.G. Martin** [***] **N. Bouraqadi** [*] **L. Etienne** [*]
K. Langueh [*] **L. Rajaoarisoa** [*] **G. Lozenguez** [*] **L. Fabresse** [*]
J.M. Maestre [***] **E. Duviella** [*]

[*] *IMT Nord Europe, Institut Mines-Télécom, Centre for Digital Systems, F-59000 Lille, France*
[**] *Instituto de Desarrollo Tecnológico para la Industria Química (INTEC), Consejo Nacional de Investigaciones cientficas y tecnicas (CONICET), Santa Fe, Argentina*
[***] *Departamento de Ingeniería de Sistemas y Automática, Universidad de Sevilla, C/ Camino de los Descubrimientos, s/n., 41092 Sevilla, Spain*

Abstract: Acquiring vast and reliable data of physicochemical parameters is critical to environment monitoring. In the context of water quality analysis, data collection solutions have to overcome challenges related to the scale of environments to be explored. Sites to monitor can be large or remote. These challenges can be approached by the use of Unmanned Vehicles (UVs). Robots provide both flexibility on intervention plans and technological methods for real-time data acquisition. Being autonomous, UVs can explore areas difficult to access or far from the shore. This paper presents a nonlinear Model Predictive Control (MPC) for UV-based exploration. The strategy aims to improve the data collection of physicochemical parameters with the use of an Unmanned Surface Vehicle (USV) targeting water quality analysis. We have performed simulations based on real field experiments with a SPYBOAT® on the Heron Lake in Villeneuve d'Ascq, France. Numerical results suggest that the proposed strategy outperforms the schedule of mission planning and exploration for large areas.

Keywords: Nonlinear MPC, Unmanned Vehicles, Environmental Missions, Water Quality Assessment

1. INTRODUCTION

The problem that we consider is that of exploration missions, which implies both mission planning and design of autonomous control strategies (Nigam, 2014).

Exploration requires offline and online motion planning, i.e., a sequence of connected linear tracks covering the entire region to explore. Most existing planners fail to incorporate multiple decision criteria and constraint such as variable length, angle and velocity trajectory segments Wu et al. (2010). In Goerzen et al. (2010) a complete overview of the existing motion planning algorithms is provided.

In case the motion planning is solved offline, the parameterized reference allows the USVs to navigate several desired regions by an autonomous control strategy. A popular control technique of growing successes, particularly in the field of MPC, is the path-following problem. A thorough review of Nonlinear MPC trajectory tracking and path-following controllers with application to nonholonomic robots can be found on Nascimento et al. (2018); Nascimento and Saska (2019). On the other hand, for exploration missions performed by multitarget tracking, there are several control designs adapted for specific environments to provide an energy efficient and robust solution. For instance, Sarunic and Evans (2014) provides a hierarchical MPC that enables an efficient trajectory for the UAVs; a nonlinear MPC scheme for navigation for constrained enviroment is proposed in Lindqvist et al. (2020); Prodan et al. (2013) (the last paper provide a path design via differential flatness); Bertrand et al. (2014) presents a framework for the cooperative guidance of a fleet of autonomous vehicles with optimal trajectories obtained for an exploration mission on a grid zone. A full discussion about the general relation between different control objectives, covering set-point stabilization, trajectory tracking, path-following and their approaches within the nonlinear MPC framework are included in Matschek et al. (2019). Although interesting, the aforementioned works and the most literature on MPC for exploration are based on set-point stabilization and the benefits of the set-based MPC (i.e., general invariant set stabilization) on the exploration missions have not been explore.

The stabilization of target sets instead of single points is more suitable in cases where it is enough to reach at least one state inside a target region. Such is the case of water resource management, where the exploration mission usually aims to cover large surface of water with an USV to visit regions where a measurement needs to be acquired (Anderson et al., 2022). In this scenario, the properties of invariant sets are useful to provide robustness, flexibility, extension of the domain of attraction, between other benefits. The set stabilization can be framed in the context of set-based MPC (Blanchini and Miani, 2015; Anderson et al., 2018) where a general invariant set is considered as a control objective.

In this context, the main contribution of this article is to present a novel set-based MPC formulation for nonlinear systems for exploration large areas with an USV. The proposal is based on a set of meshing of the region to be explored with a twofold aims, to configure a simple motion planning offline for the problem and to use the sets composing the meshing as target sets for the controller. Several simulation results targetting water quality assessment show the properties of the proposed controller.

The structure of this paper is as follows. Section 2 present the nonlinear system and some basic concepts of the regions of the state space. Section 3 describes the general set-based MPC formulation and some stability conditions. The main result of the paper is presented in Section 4. In this section the proposal is formulated and some simulation results show its properties. The nonlinear model and the properties of the USV are stated on Section 5.1. In Section 6 the problem statement of the water quality assessment is presented and the simulation results are presented. Lastly, Section 7 states the conclusions of the paper.

1.1 Notation

We denote with $\mathbb{N}$ the sets of integers, $\mathbb{N}_0 := \mathbb{N} \cup \{0\}$ and $I_i := \{0, 1, \ldots, i\}$. The ceiling function is defined by $\text{ceil}(x) := \min\{n \in \mathbb{N} : x \leq n\}$. Consider two sets $\mathcal{U} \subset \mathbb{R}^n$ and $\mathcal{V} \subset \mathbb{R}^n$, containing the origin and a real number λ. The Minkowski sum $\mathcal{U} \oplus \mathcal{V} \subset \mathbb{R}^n$ is defined by $\mathcal{U} \oplus \mathcal{V} = \{(u + v) : u \in \mathcal{U},\ v \in \mathcal{V}\}$; the set $\mathcal{U} \setminus \mathcal{V} \subset \mathbb{R}^n$ is defined as $\mathcal{U} \setminus \mathcal{V} = \{u : u \in \mathcal{U} \wedge u \neq \mathcal{V}\}$; and the set $\lambda\mathcal{U} = \{\lambda u : u \in \mathcal{U}\}$ is a scaled set of $\mathcal{U}$. The *close ball with center in* $x \in \mathbb{R}^n$ *and radius* $\varepsilon > 0$ is given by $\mathcal{B}(x, \varepsilon) := \{y \in \mathbb{R}^n : \|x - y\| \leq \varepsilon\}$. The point x is an *interior point of* $\mathcal{U}$ if the there exists $\varepsilon > 0$ such that the open ball $\mathcal{B}(x, \varepsilon) \subseteq \mathcal{U}$. The interior of a set $\mathcal{U}$ is the set of all its interior points and it is denoted by $\text{int}\,\mathcal{U}$.

2. NONLINEAR SYSTEM AND PRELIMINARY ANALYSIS

The dynamic process discussed in this work consists in the class of discrete-time nonlinear system described by the following equations

$$\begin{cases} x(i+1) & = f(x(i), u(i)), \\ x(0) & = x_0, \end{cases} \tag{1}$$

where $x(i) \in \mathbb{X} \subset \mathbb{R}^n$ represents the measured states of the system and $u(i) \in \mathbb{U} \subset \mathbb{R}^m$ the control input at time i. The constraint sets $\mathbb{X}$ and $\mathbb{U}$ are compact and convex with the origin inside, and the function $f : \mathbb{X} \times \mathbb{U} \to \mathbb{X}$ is continuous with $f(0, 0) = 0$.

The general permanence regions of a dynamical system (i.e., equilibrium manifolds or invariant sets) are quite meaningful to characterize stable regions as control objectives for a controlled system (Blanchini and Miani, 2015). The following definition presents the concept of invariance sets - generally used as target sets in the set-based MPC context - which are defined by transient states of the system that can remain indefinitely in the same region by mean of admissible inputs.

Definition 1 (Control Invariant Set - CIS)**.** *The set* $\Omega \subset \mathbb{X}$ *is a control invariant set (CIS) for system* (1) *if for all* $x \in \Omega$ *there exists* $u \in \mathbb{U}$ *such that* $f(x, u) \in \Omega$*.*

The CIS has an associated corresponding input set given by

$$\Psi(\Omega) := \{u \in \mathbb{U} : \exists\, x \in \Omega \text{ such that } f(x, u) \in \Omega\},$$

meaning that every input on $\Psi(\Omega)$ leaves at least one state of Ω inside Ω.

A CIS is called a Contractive CIS if the condition on Definition 1 is replaced by: for every $x \in \Omega$ there is $u \in \mathbb{U}$ such that $f(x, u) \in \text{int}\,\Omega$.

The asymptotic stability of sets rather than equilibrium points allows to robustly generalized target regions, this is useful when the solutions of the dynamical system cannot be settled down into an single point, which frequently happens due to the uncertainties, or the timer variable does not converge to a point but rather to an interval (such as the case with sample-and-hold control systems).

3. SET-BASED MPC

A generalization of the MPC controller for tracking invariant sets is presented. The idea is to track and reach sets that not only include stationary states, but also transient states. We start with a quite general formulation, that is particularized in the next subsections to different applicable cases. Also consider the following definition.

Definition 2 (Generalized Distance Stage Cost Function)**.** *A generalized distance function* $d(x, \Omega)$*, from* x *to the CIS* Ω*, is a function with the following properties: (1)* $d(x, \Omega)$ *is convex and continuous for all* $x \in \mathbb{X}$*, (2)* $d(x, \Omega) = 0$ *for all* $x \in \Omega$*, (3)* $d(x, \Omega) > 0$ *for all* $x \in \mathbb{X} \setminus \Omega$*.*

The proposed controller cost function will be given by:

$$V_N(x, \Omega; \mathbf{u}) = \sum_{j=0}^{N-1} \alpha d(x_j, \Omega) + \beta d(u_j, \Psi(\Omega)), \tag{2}$$

where α and β are positive real numbers, N is the prediction horizon, the initial state $x = x_0$, the predicted states $x_{j+1} = f(x_j, u_j)$ and the input sequence $\mathbf{u} = \{u_0, \cdots, u_{N-1}\}$.

Remark 3. *The usual terminal cost associated with the terminal predicted state* x_N *can be omitted on Eq.* (2) *if* x_N *is force to belong to the set* Ω*, i.e.,* $d(x_N, \Omega) = 0$*. As usual in MPC design, a local control action* $\bar{u}$ *that will act for predictions inside the terminal set* Ω *will have also null cost since* $\bar{u} \in \Psi(U)$*.*

The general set-based MPC is given by the following optimization problem solved at each sample time $k \in \mathbb{N}$.

$$\begin{aligned} & \min_{\mathbf{u}} V_N(x, \Omega; \mathbf{u}) \\ \text{s.t.} \quad & x_0 = x, \\ & x_{j+1} = f(x_j, u_j), \quad j \in I_{N-1}, \\ & x_j \in \mathbb{X}, \quad u_j \in \mathbb{U}, \quad j \in I_{N-1}, \\ & x_N \in \Omega \end{aligned} \tag{3}$$

Taking into account the receding horizon policy, the control law at time k is given by the first element of the optimal sequence $\mathbf{u}^o$ of the optimization problem given by (3) solved at time k.

Consider the next Lemma for the asymptotic stability of the closed-loop system.

Lemma 4. *If* $\Omega \subset \mathbb{X}$ *is a CIS for system* (1) *in the cost function* (2)*, then* Ω *is asymptotic stable for the closed-loop system* (1) *controlled by the set-based MPC given by* (3)*.*

Proof. The proof can be found on Blanchini and Miani (2015). It is stated that under the hypothesis of the Lemma there is a Lyapunov function (given by the optimal cost $V_N^0(\cdot)$) that is a

decreasing function on the level sets of the generalized distance function used on the function cost (see Fig. 1 and 2). □

Provided that the MPC formulation is strongly based on the concept of generalized distance functions, two possible candidates that fulfills Definition 2 will be presented below.

Definition 5. *Given a CIS Ω, the matrix distance from x to Ω is defined as*

$$d(x, \Omega) = \min_{y \in \Omega} \|x - y\|_M^2, \quad M > 0$$

The Minkowski functional (Blanchini and Miani, 2015) is defined as:

Definition 6. *Given a CIS Ω, the Minkowski functional Φ_Ω associated to Ω is defined as*

$$\Phi_\Omega(x) = \inf\{\mu \geq 0 : x \in \mu\Omega\}.$$

The Minkowski functional has a number of useful properties (Blanchini and Miani, 2015). It also was already used as a part of MPC costs in works as Raković and Lazar (2012); González et al. (2011). However, the Minkowski functional is not null inside the set to which it is associated. To achieve this property, we need to introduce the modified Minkowski functional.

Definition 7. *Given a convex set Ω, that includes the origin as an interior point, and a contractive Invariant Set Σ for the autonomous system $x(i+1) = f(x(i), x \in \mathbb{X}$, the modified Minkowski functional is defined as*

$$\bar{\Phi}(x) = \inf\{\mu \geq 0 : x \in \Omega \oplus \mu\Sigma\}.$$

Property 8. *The distance from a point to a set defined by the functions on Definition 5 and 7 satisfies the properties of a generalized distance stage cost function from Definition 2.*

Proof. The proof can be found on González et al. (2014). □

Fig. 1 and 2 shows a schematic plots of a Distance function and the Modified Minkowski functional associated to an arbitrary polytopic set, respectively, together to the level sets where the optimal cost is a decreasing function. Notice that inside the set the functions are null.

Next section presents an extension of the set-based MPC to tracking multi-target sets.

3.1 Multi-target tracking

In what follows the control formulation presented on the last section is extended for tracking multi-target sets.

Consider that the closed-loop system has to reach every element on the set $\mathbf{\Omega} = \{\Omega_1, \Omega_2, \cdots, \Omega_K\}$ with $\Omega_i \subset \mathbb{X}$ for $i = 1, \cdots, K$, in the specified order. This is, once the controlled system reaches the target set $\Omega_j \in \mathbf{\Omega}$, the objective change to Ω_{j+1} and so on until the state of the system converge to Ω_K. Clearly, a condition must be establish in order to switch target every time the current target is reached. In the MPC framework, there are several strategies to approach this goal, such as event-triggered MPC Tabuada (2007), switched MPC, dual-MPC, etc. However, in our case a state-dependent MPC will be used, in this context a condition to consider a reached target set that it depends on the current state position is established.

Definition 9 (Reached set)**.** *The first set on $\mathbf{\Omega}$, i.e., Ω_1 is considered a* reached set *if $x(i) \in \Omega_1$ for some $i > 0$. For $k > 1$, the target set $\Omega_k \in \mathbf{\Omega}$ is considered a* reached set *if $x(i) \in \Omega_k$ for some $i > 0$ and the previous sets $\Omega_1, \ldots, \Omega_{k-1}$ are* reached sets.

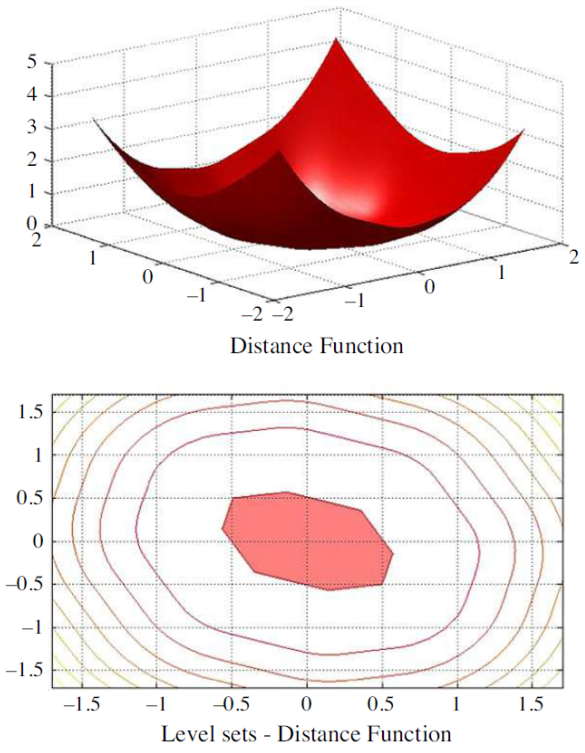

Fig. 1. Descriptive plot of the Distance Function associated to a given set.

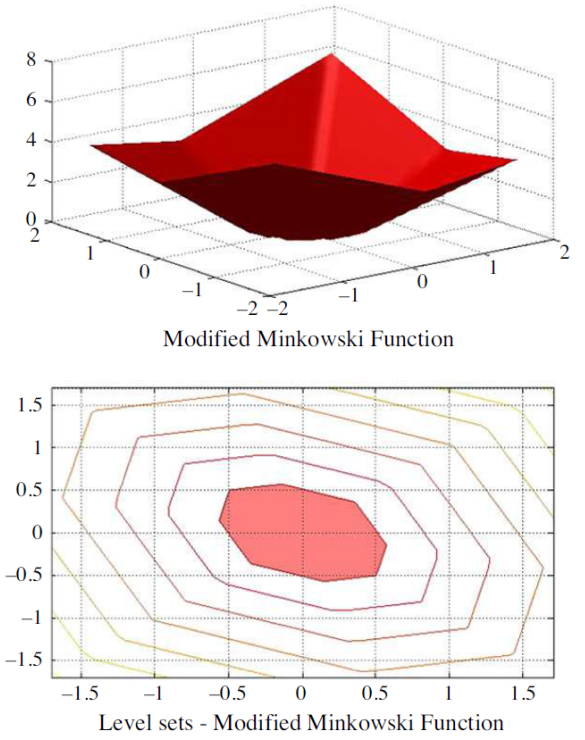

Fig. 2. Descriptive plot of the Modified Minkowski Functional associated to a given set.

As it can be seen, the condition for a set on $\mathbf{\Omega}$ to be a *reached set* is defined inductively.

Now, consider the following target set depending on the position of the state x, Ω_x, given by the following.

Definition 10 (Current target set)**.** *Given the sates of the closed-loop system $x(i) \in \mathbb{X}$ for $i = 0, \dots, T$, where $x = x(T)$ is the current state. The current target set is given by*

$$\Omega_x := \{\Omega_{k+1} : k = \max\{i : \Omega_i \text{ is a reached set}\}\} \quad (4)$$

In the case that there is not reached sets then $\Omega_x := \Omega_0$.

In simple words, Ω_x it defines which is the current objective depending on the position of the state $x \in \mathbb{X}$.

The next MPC formulation to tracking target sets is based on the results proposed by Limon et al. (2005), where the tracking of reachable sets where used to extend the domain of attraction of the controller.

Considering the control law derived from solving by the receding horizon strategy the following optimization problem.

$$\begin{aligned} \min_{\mathbf{u}} & V(x, \Omega_x, \mathbf{u}) \quad (5)\\ \text{s.t.} \quad & x_0 = x, \\ & x_{j+1} = f(x_j, u_j), \quad j \in I_{N-1}, \\ & x_j \in \mathbb{X}, \quad u_j \in \mathbb{U}, \quad j \in I_{N-1}, \\ & x_N \in \Omega_x, \end{aligned}$$

For an asymptotic stability condition consider the next Lemma.

Lemma 11. *If $\Omega_j \in \mathbf{\Omega}$ is a Contractive CIS for all $j = 1, \dots, K$, then every $\Omega_j \in \mathbf{\Omega}$ is a reached set for the closed-loop system controlled by the MPC given on* (5)*.*

Proof. If the current target set $\Omega_x = \Omega_j$ is a Contractive CIS for system (1), the results proposed on Anderson et al. (2018) proves that the closed-loop system will reach in finite-time the set Ω_x. Therefore, according the formulation, once the target set Ω_j is reached, the current state switch to $\Omega_x = \Omega_{j+1}$. The proof is concluded by induction. □

The above Lemma highlights the fact that the asymptotic stability of every set $\Omega_j \in \mathbf{\Omega}$ is not enough to guarantee that every set on $\mathbf{\Omega}$ is reached. To fulfill every objective a guarantee of finite-time convergence of every Ω_j is necessary.

The following section provides the main result of the paper. The proposal is an extension of the above MPC formulation that aims to improve the performance of the controlled trajectory.

4. PROPOSED MPC

In this section, the MPC based on sets for tracking multi-target set is extended to improve performance. The extension is based on tracking two consecutive sets on the path $\mathbf{\Omega} = \{\Omega_1, \dots, \Omega_K\}$, i.e., part of the predictions attempt to reach the current target set $\Omega_x = \Omega_j$ and the rest of the predictions attempts to reach the target set Ω_{j+1}. This way, the control design plans the approach to Ω_j taking into account that the next step is to reach the set Ω_{j+1}.

To this end a dual-MPC is formulated, where the goal of the first mode is to reach only the current target set $\Omega_x = \Omega_j$, by means of (5). The second mode is activated by the time the current state x is close enough of Ω_x, this mode considers as part of the objective the target set Ω_{j+1}, so the trajectory to reach Ω_x takes into account the next steps to reach Ω_{j+1}.

To trigger the second mode the current state must be close enough of Ω_x. This condition can be stated by the inclusion of the current state on the fattening set of Ω_x.

Definition 12 (Fattening set)**.** *Let $\Omega_x \subset \mathbb{R}^n$ be the current target set of control, and let $\varepsilon > 0$, we denote the ε-*fattening set of Ω_x *by*

$$(\Omega_x)^\varepsilon := \cup\{\mathcal{B}(x, \varepsilon) : x \in \Omega_x\}.$$

Remark 13. *The term 'close enough' of the current target set is a parameter of the control design and can be selected by chosen an appropriate ε.*

The second mode is activated when the current state is on $(\Omega_x)^\varepsilon$, at this time the design of the control consider the next target set, i.e. if $\Omega_x = \Omega_j$ then the next target set is Ω_{j+1}. To properly define this next objective depending on the current state, consider the following definition.

Define Ω_x as in Eq. (4), and the set Ω_x^+ as follows:

$$\Omega_x^+ := \begin{cases} \Omega_{j+1}, \text{ being } \Omega_j = \Omega_x, & x \in (\Omega_x)^\varepsilon \\ \Omega_x, & \text{otherwise} \end{cases} \quad (6)$$

Note that, if the current state $x \notin (\Omega_x)^\varepsilon$, then it is considered that $\Omega_x^+ = \Omega_x$. This detail allows to formulate the problem in a consistent way.

Consider now the function $N_x : \mathbb{X} \to \mathbb{I}_N$ that defines the prediction of horizon of the proposed controller:

$$N_x := \begin{cases} \text{ceil}(\frac{Nd(x,\Omega_x)}{\varepsilon}), & x \in (\Omega_x)^\varepsilon \\ N, & \text{otherwise} \end{cases}$$

Note that for the first mode, i.e. when $x \notin (\Omega_x)^\varepsilon$, the prediction horizon is N. For the second mode, i.e. when $x \in (\Omega_x)^\varepsilon$, the prediction horizon decreases with the distance of the current state x to the current target set. The $\text{ceil}(\cdot)$ function is considered for N_x to be an integer number.

Remark 14. *Function N_x is a decreasing function with maximum value when x belongs to the boundary of $(\Omega_x)^\varepsilon$, given by $N_x = N$; and a minimum value when $x \in \Omega_x$, given by $N_x = 0$.*

The second mode computes N_x predicted states that attempt to reach Ω_x, and $N - N_x$ predicted states that attempt to reach Ω_x^+. Note that, when $x \to \Omega_x$, $N_x \to 0$, and most of predictions are used to reach the set Ω_x^+.

The cost function is given by

$$J_N(x; \mathbf{u}) = \sum_{j=0}^{N_x - 1} p\ell_{\Omega_x}(x_j, u_j) + \sum_{j=N_x}^{N-1} q\ell_{\Omega_x^+}(x_j, u_j) \quad (7)$$

where $\ell_\Omega(x_j, u_j) := \alpha d(x_j, \Omega) + \beta d(u_j, \Psi(\Omega))$, and $p, q > 0$ are weight values.

The nonlinear MPC is given by the following optimization problem solved at each sample time $k \in N$.

$$\min_{\mathbf{u}} \; J_N(x;\mathbf{u}) \tag{8}$$
$$\begin{aligned} \text{s.t.} \quad & x_0 = x, \\ & x_{j+1} = f(x_j, u_j), \quad j \in I_{N-1}, \\ & x_j \in \mathbb{X}, \quad u_j \in \mathbb{U}, \quad j \in I_{N-1}, \\ & x_{N_x} \in \Omega_x, \\ & x_N \in \Omega_x^+, \end{aligned}$$

The solution of Problem (8) is the optimal control sequence $\mathbf{u}^0 = \{u_0^0, u_1^0, \cdots, u_{N-1}^0\}$. Taking into account the receding horizon policy, the control law at time i is given by $\kappa = u_0^0$ (the first element of the optimal control sequence), which is applied to the real plant at every time step i.

The control algorithm executed at any $i-th$ time instant is the following:

Algorithm 1: Proposed nonlinear MPC algorithm

Data: $N \in \mathbb{N}, \mathbb{X} \subset \mathbb{R}^n, \mathbb{U} \subset \mathbb{R}^m, \mathbf{\Omega} = \{\Omega_j\}_{j=1}^K$
Result: Closed-loop system $x(i+1) = f(x(i), \kappa(i))$
1: Read $x = x(i)$;
2: Compute Ω_x, Ω_x^+ with Eq. (4) and (6);
3: Solve Problem (8);
4: Inject $\kappa(i) = u_0^0$ into the system;
5: $i \leftarrow i + 1$;
6: Go back to 1

The dual-behaviour of optimization problem (8) is given by two modes; the first mode is activated when $x \notin (\Omega_x)^\varepsilon$ and is easy to prove that (8) is equivalent to (5), so the problem is reduce only to track the current target set, i.e. Ω_x. The second mode is activated when the system is near to the current target set, i.e. $x \in (\Omega_x)^\varepsilon$, in this mode the system is driven to the current target set Ω_x considering that once there the next target set is Ω_x^+.

Remark 15. *A general strategy of the proposal can be stated with more than two simultaneous target sets on* $\mathbf{\Omega}$*, this could be appropriate when the target sets are very close each other. However this extension implies further analysis.*

4.1 Some quantitative properties of the proposal

In what follows, some numerical results are shown to clarify the nontrivial properties of the proposed controller.

We consider the USV model represented by Eq. (10). With abuse of notation let define the current state of the vessel by

$$x(i) = (x, y, \psi, u, v, r),$$

for every time $i \geq 0$. Where x, y, z represent position sates, on the surface (x, y) and ψ is the 'direction position' of the vehicle in the inertial frame. Meanwhile u, v, r represent the velocities states, i.e., surge (forward), sway (perpendicular) and yaw (angular), respectively.

The first simulations attempts to show the anticipatory behaviour of the proposed control. Consider the paths given by $\mathbf{\Omega} = \{\Omega_1, \cdots, \Omega_5\}$ and $\mathbf{\Psi} = \{\Psi_1, \cdots, \Psi_5\}$ on the surface of the water (see Fig. 3). This two paths are a reflection of each other.

Note that both controlled trajectories of the vessel are the same until the USV is 'close enough' of the first target set in order to activate the second mode of the control. At this point, both

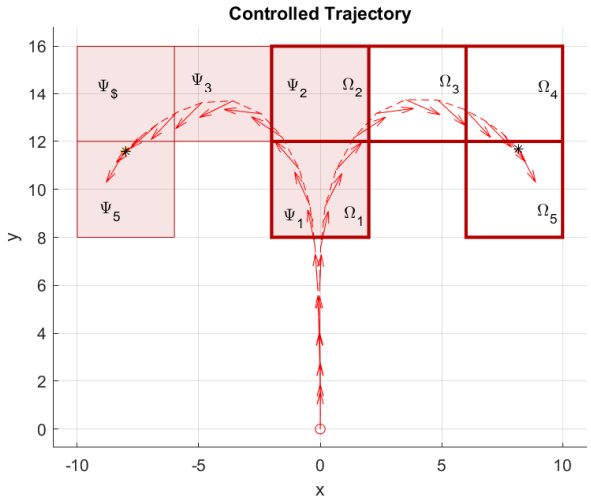

Fig. 3. Two different controlled trajectories to follow path $\mathbf{\Omega}$ and path $\mathbf{\Psi}$.

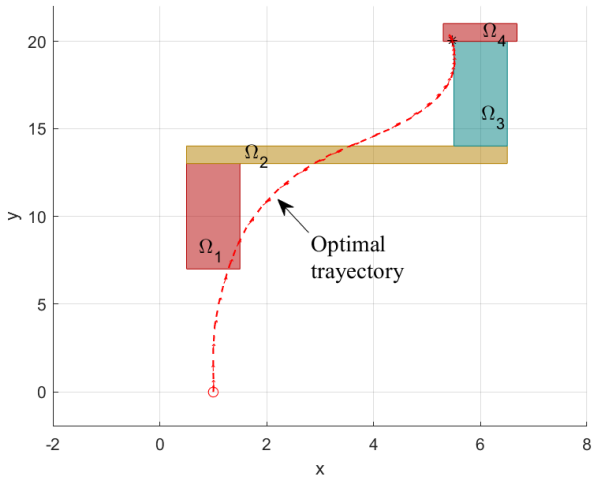

Fig. 4. Optimal trajectory that pass over every target set Ω_j $j = 1, \ldots, 4$.

trajectories take different directions according the orientation of the path that is followed. This anticipatory behaviour remains until the vessel reaches the last target set on every path.

Consider now the scenario presented on Fig. 4. The objective is to drive the initial state $x(0) = (0, 0, \frac{pi}{2}, 0, 0, 0)$ to Ω_1, from there to Ω_2 then to Ω_3 and finally to Ω_4. There are infinite trajectories and countless strategies to fulfill this objective, however the optimal trajectory - given by proposed strategy - selects the optimal position to pass through Ω_j considering that from there the system need to be driven to Ω_{j+1}, for $j = 1, \ldots, 3$. It is noteworthy that the optimal trajectory reaches only the boundary of Ω_3, since it is enough to reach the last target set Ω_5 from there.

Remark 16 (Dimension of target sets Ω_j)**.** *Note that by definition the dimension of the target sets* $\Omega_j \in \mathbb{X}$ *matches with the dimension of the states. In the above examples the sets* Ω_j *belongs to the surface* (x, y)*, however to accomplish the real dimension of the set the following set was considered*

$$\Omega_j = \{(x, y, \psi, u, v, r) \in \mathbb{R}^6 : \; l_x \leq x \leq u_x, \; l_y \leq y \leq u_y, \ldots \tag{9}$$
$$\infty \leq \psi, u, v, r \leq \infty\}.$$

In the water quality application problem assessed on Section 6 the target sets Ω_j belongs to $/R^3$, two dimension for the surface (x, y) and one more for the forward velocity state u.

5. SPYBOAT®'S DESCRIPTION

In this section the description of the USV used on the simulation results and the real experiment described on Section 6 is presented.

The CT2MC company has designed a range of vessels dedicated to answer the need of data monitoring of freshwater resource. The main feature of these vehicles consists in a flat hull and aerial propulsion system that it guarantees the realization of sampling missions and inspections without contamination of the environment.

The SPYBOAT® technology follows standard equipment configuration including multiple sensors (localization system, compass, sonar, camera) and is propelled by two independent actuators. Thus the heading is controlled through a differential thrust method. The architecture of the SPYBOAT® technology is described in Fig. 5.

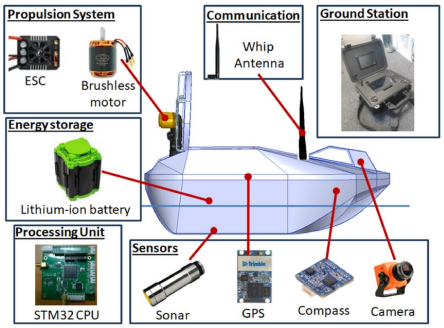

Fig. 5. Architecture of SPYBOAT® technology.

The USV is equipped with a *Hyperion* optical sensor from Valeport [1], for the measurement of the turbidity. It is also equipped with Tripod sensors from AquaLabo [2] to measure the temperature, Dissolved Oxygen, pH, and conductivity.

5.1 USV nonlinear system

In Hervagault (2019) a kinematic model for the SPYBOAT® vessel was identified based on the following standard assumptions.

Assumption 17 (Liu et al. (2016)). *(i) USVs are moving in a horizontal plane in an ideal fluid. (ii) USV masses are uniformly distributed. (iii) The CG and center of buoyancy (CB) point vertically along the z-axis. (iv) USVs have port-starboard symmetry. (v) Surge and sway-yaw dynamics are essentially decoupled.*

In addition to the standard assumptions, the characteristics of the SPYBOAT® vessel allows to consider the following.

[1] https://www.valeport.co.uk/content/uploads/2021/05/0901814i-Hyperion-Optical-Sensors-Operating-Manual.pdf
[2] https://en.aqualabo.fr/

Assumption 18 (Hervagault (2019)). *We will consider the fore/aft symmetry for our system. Considering their flat hull, they don't present any stem for hydro-dynamical optimization. So the Inertia and Damping matrices can be simplified by canceling their off-diagonal terms. Furthermore, in the control model, the non-linear damping will be considered as an external disturbance.*

The marine craft moves on an horizontal plane and only surge, sway and yaw are considered. The resulting is a nonlinear model given by the following equations.

$$\begin{cases} \dot{x} &= u\cos(\psi) - v\sin(\psi), \\ \dot{y} &= u\sin(\psi) + v\cos(\psi), \\ \dot{\psi} &= r, \\ \dot{u} &= \frac{\tau_u}{m_{11}} + \frac{m_{22}}{m_{11}} vr + \frac{X_u}{m_{11}} u, \\ \dot{v} &= -\frac{m_{11}}{m_{22}} ur + \frac{Y_v}{m_{22}} v, \\ \dot{r} &= \frac{\tau_r}{m_{33}} + \frac{m_{22}-m_{11}}{m_{33}} uv + \frac{N_r}{m_{33}} r \end{cases} \tag{10}$$

The vector (x, y) is the position on the surface and ψ the direction of the vessel, u, v, r are the surge, sway and yaw velocities respectively. The inputs are given by $\tau_u = F_1 + F_2$ and $\tau_r = b(F_1 - F_2)$, where F_1 and F_2 are the port side and starboard side thrust forces, and b represent $1/2$ of the distance between thrusters. The parameter X_u, Y_v and N_r are the linear drag coefficient in surge direction from surge, the linear drag coefficient in sway direction from yaw rate and the linear drag moment coefficient from yaw rate, respectively. The mass parameters m_{ii} include added mass contributions that represent hydraulic pressure forces and torque due to forced harmonic motion of the vessel which are proportional to acceleration:

$$\begin{aligned} m_{11} &= m + 0.05m, \\ m_{22} &= m + 0.5(\rho\pi D^2 L), \\ m_{33} &= \frac{m(L^2 + W^2) + 0.5(0.1mB^2 + \rho\pi D^2 L^3)}{12}. \end{aligned}$$

where m is the actual mass, L is the effective length (hull's length in the water), W is the width, D is the mean submerged depth, B is the distance between propellers and ρ is the water density.

For more detail on the parameters of model (10) see Hervagault (2019).

6. APPLICATION TO ENVIRONMENTAL MISSIONS

In this section some simulation results for exploration mission targetting water quality map extraction are presented. First, the problem statement and the general objective of the mission are explained.

6.1 Problem statement

In Anderson et al. (2022), a data collection of physicochemical parameters (such as pH, turbidity, conductivity, temperature and dissolved oxygen) that indicate the pollution index of water surface were studied in a particular region of the Heron Lake in Villeneuve d'Ascq, France (see region Ω on Fig. 6). In this artificial lake the water arrives from east and when the level is too high water is pumped out to a nearby river in the far western point. A natural remediation of the water occurs in lake so a gradient of the parameters can be expected between points on

the entrance with a high biodegradable inputs (Ivanovsky et al., 2018).

Fig. 6. Region Ω on the Heron lake, Villeneuve d'Ascq, where the measurements need to be acquire.

Remark 19 (General objective)**.** *In this context - as was explain on Anderson et al. (2022) - the general objective is to construct a limnological map of the region Ω, i.e., a map* $F : \Omega \to \mathbb{R}^5$ *such that* F *assigns to every point on* Ω *its approximation value of pH, turbidity, conductivity, temperature and dissolved oxygen (see Fig. 8 for dissolved oxygen).*

The construction of map F on the region of interest was discussed on Anderson et al. (2022), where an approximation of F was proposed by geo-statistical interpolation methods based on real measurements provided by a hand-operated USV. The interpolation method was necessary at this point in order to complete uncovered points (unmeasured positions) due to the irregularity of the hand-operated trajectory (see Fig. 7).

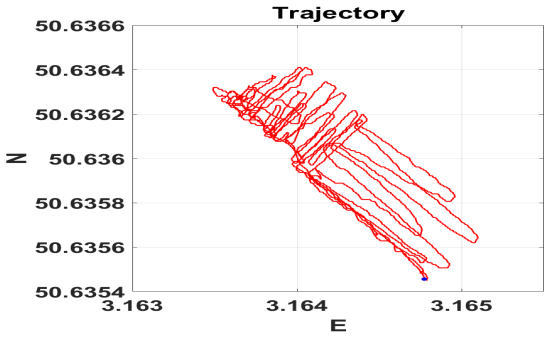

Fig. 7. Trajectory of the hand-operated vessel in region Ω with decimal GPS coordinates.

To improve the data collection of the aforementioned physic-ochemical parameters, in what follows the proposed control strategy is performed for a regular exploration of region Ω.

6.2 Motion planning

The area of interest Ω was computed by the largest convex set containing the entire data collection of Fig. 8. The design of the path to explore the complete region is based on a regular map meshing of Ω. The map meshing consists in a collection of disjointed sets $\{\Omega_j\}_{j=1}^{K}$ such that $\cup\Omega_j$ contains the region Ω. The size of every Ω_j must be considered according the size of the vessel, the accurate of the map F, the time for the exploration mission, etc. On the other hand, the shape of Ω_j must be chosen according the best performance of the

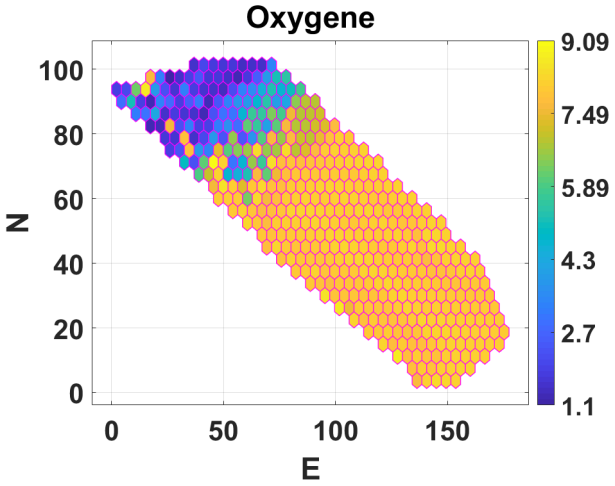

Fig. 8. Limnological map F on Ω for the Dissolved Oxygen (Anderson et al., 2022).

controller. Figure 9 shows a motion planning for squares Ω_j with a size of $100m^2$. A discussion about the shapes and sizes of the meshing is discussed on Anderson et al. (2022)

The controlled vessel reaches every set Ω_j and performes a direct in situ measurement of each parameters. The limnological map F is constructed by this process.

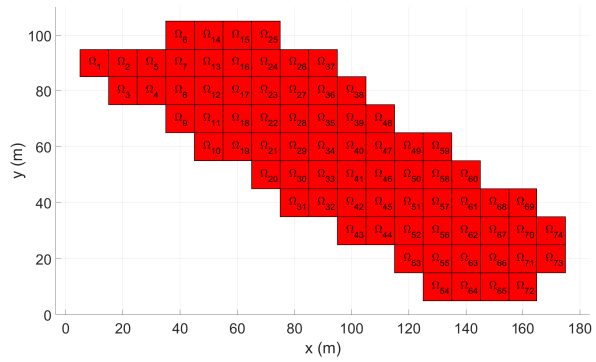

Fig. 9. A motion planning to explore Ω.

Remark 20. *The path* $\mathbf{\Omega} = \{\Omega_1, \cdots, \Omega_K\}$ *is an ordered sequence that determine in which order the target sets* Ω_j *are reached. According to the meshing considered in this work, there are several possible regular paths for exploration; a proper motion path would depends on the position of the initial state, wind, water flow, etc.*

6.3 Exploring results

Fig. 10 shows the application of the proposed MPC with a prediction horizon $N = 15$, a discretization of the dynamical model (10) with discrete-time with $T = 1seg$ and initial state $x(0) = (x, y, \psi, u, v, r) = (20, 105, -\frac{pi}{2}, 0, 0, 0)$. To explore region Ω a regular meshing of squares with a size of $25m^2$ is used. Every target set Ω_x share an edge with the next target set Ω_x^+, so once the system enter into Ω, only the second mode of the MPC (8) is used (the first mode is only used at the beginning to reach Ω_1). Fig. 10 shows the controlled trajectory that reach every target set Ω_j at least one time.

In order to construct the map F by direct in situ measurements of each parameters inside every target set Ω_j, the velocity u of

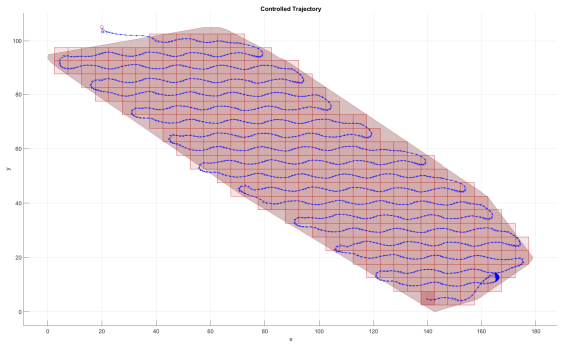

Fig. 10. Controlled trajectory for exploring region Ω.

the vessel must belongs to certain range to allows the sensor to take every measurement inside Ω_j for all $j = 1, \ldots, K$. This can be approach by considering target sets of three dimensions, i.e.

$$\Omega_j = \{(x, y, \psi, u, v, r) \in \mathbb{R}^6 : \ l_x \leq x \leq u_x, \ l_y \leq y \leq u_y, \ldots \\ l_u \leq u \leq u_u, \ \infty \leq \psi, v, r \leq \infty\}.$$

Note that there is no consideration to minimize states ψ, v and r, which means that they are free. For the simulations on Fig. 11 we consider that $1 \leq u \leq 2$ for all Ω_j, $j = 1 \ldots, K$, i.e., $\text{proj}_u \, \Omega_j = [1, 2]$ for all j. The figure shows the velocity state and inputs for the time interval $[0, 100]$. On the other hand, for the simulations on Fig. 12 the target set for the velocity is $0.5 \leq u \leq 1.5$ for all Ω_j, $j = 1 \ldots, K$, i.e., $\text{proj}_u \, \Omega_j = [0.5, 1.5]$ for all j.

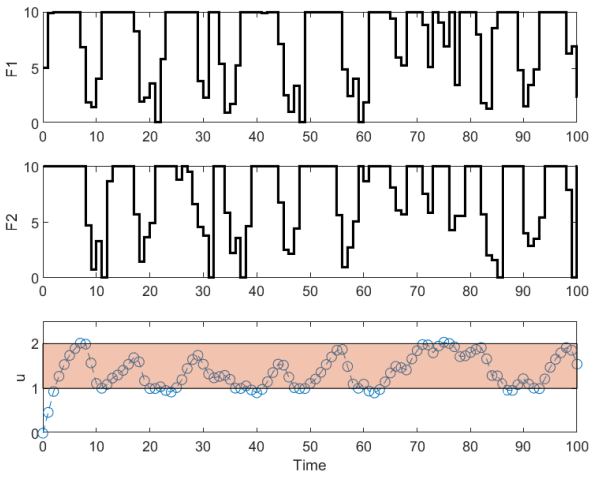

Fig. 11. Inputs and velocity state for the target set $\text{proj}_u \, \Omega_j = [1, 2]$.

Remark 21. *Simulation results suggest that the exploration of the region of interest Ω can be done with a very simple motion planing and with an optimal trajectory that reaches every point on the surface where a measurement needs to be performed. Even more, the velocity of the vessel can be selected for every target Ω_j with $j = 1 \ldots, K$ according the requirements of the experiment. However, more simulation experiments need to be done before the real implementation, but they are out of the scope of this work.*

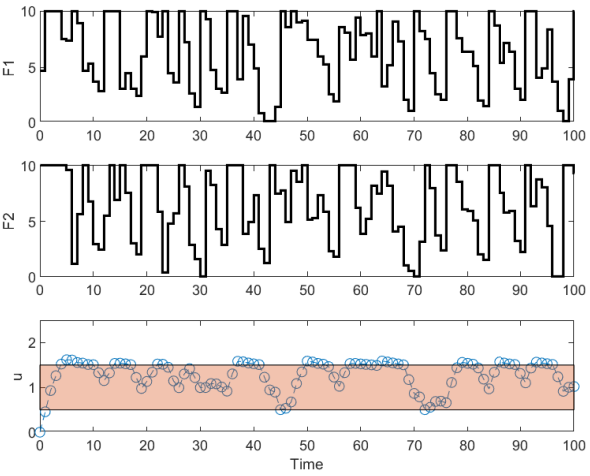

Fig. 12. Inputs and velocity state u for the target set $\text{proj}_u \, \Omega_j = [0.5, 1.5]$.

7. CONCLUSION

Environmental missions were performed on Heron Lake in Villeneuve d'Ascq, France. The main goal of the experiment is to construct a temporal water quality profile of a region of the lake, where there is a suspicion of a source of pollution, so more experiments are expected in the same region. To outperformed the data collection results, in this paper a nonlinear MPC for USV for exploration was presented. The strategy shows that a simple schedule of mission planning can be obtained, and the simulations proves that large water surfaces can be tracked in an optimal and flexible way. This results are expected to outperformed the real exploration of large areas targeting data collection for water quality analysis.

ACKNOWLEDGMENT

Authors want to thanks the company Bathy drone Solutions (BDS) for its participation in the experiments, and the Department of Economic Transformation, Industry, Knowledge and Universities of the Andalusian Government (PAIDI 2020) [Ampliación Aquacollect, ref. P18-HO-4713].

REFERENCES

Anderson, A., Martin, J., Mougin, J., Bouraqadi, N., Duviella, E., Etienne, L., Fabresse, L., Langueh, K., Lozenguez, G., Alary, C., Billon, G., Superville, P., and Maestre, J. (2022). Water Quality Map Extraction from Field Measurements Targetting Robotic Simulations. URL `https://hal.archives-ouvertes.fr/hal-03610878`. Working paper or preprint.

Anderson, A., González, A.H., Ferramosca, A., and Kofman, E. (2018). Finite-time convergence results in robust model predictive control. *Optimal Control Applications and Methods*, 39(5), 1627–1637.

Bertrand, S., Marzat, J., Piet-Lahanier, H., Kahn, A., and Rochefort, Y. (2014). MPC strategies for cooperative guidance of autonomous vehicles. *Aerospace Lab*, (8), 1–18.

Blanchini, F. and Miani, S. (2015). *Set-Theoretic Methods in Control*. Systems & Control: Foundations & Applications. Springer International Publishing. URL

https://books.google.com.ar/books?id=8a0YCgAAQBAJ.

Goerzen, C., Kong, Z., and Mettler, B. (2010). A survey of motion planning algorithms from the perspective of autonomous uav guidance. *Journal of Intelligent and Robotic Systems*, 57(1), 65–100.

González, A., Adam, E., Marcovecchio, M., and Odloak, D. (2011). Stable mpc for tracking with maximal domain of attraction. *Journal of Process Control*, 21(4), 573–584.

González, A.H., Ferramosca, A., Bustos, G.A., Marchetti, J.L., Fiacchini, M., and Odloak, D. (2014). Model predictive control suitable for closed-loop re-identification. *Systems & Control Letters*, 69, 23–33.

Hervagault, Y. (2019). *Design and Implementation of an Effective Communication and Coordination System for Unmanned Surface Vehicles (USV)*. Ph.D. thesis, Université Grenoble Alpes.

Ivanovsky, A., Belles, A., Criquet, J., Dumoulin, D., Noble, P., Alary, C., and Billon, G. (2018). Assessment of the treatment efficiency of an urban stormwater pond and its impact on the natural downstream watercourse. *Journal of Environmental Management*, 226, 120–130. doi:https://doi.org/10.1016/j.jenvman.2018.08.015. URL https://www.sciencedirect.com/science/article/pii/S0301479718308867.

Limon, D., Alamo, T., and Camacho, E.F. (2005). Enlarging the domain of attraction of mpc controllers. *Automatica*, 41(4), 629–635.

Lindqvist, B., Mansouri, S.S., and Nikolakopoulos, G. (2020). Non-linear mpc based navigation for micro aerial vehicles in constrained environments. In *2020 European Control Conference (ECC)*, 837–842. IEEE.

Liu, Z., Zhang, Y., Yu, X., and Yuan, C. (2016). Unmanned surface vehicles: An overview of developments and challenges. *Annual Reviews in Control*, 41, 71–93.

Matschek, J., Bäthge, T., Faulwasser, T., and Findeisen, R. (2019). Nonlinear predictive control for trajectory tracking and path following: An introduction and perspective. In *Handbook of Model Predictive Control*, 169–198. Springer.

Nascimento, T.P., Dórea, C.E., and Gonçalves, L.M.G. (2018). Nonholonomic mobile robots' trajectory tracking model predictive control: a survey. *Robotica*, 36(5), 676–696.

Nascimento, T.P. and Saska, M. (2019). Position and attitude control of multi-rotor aerial vehicles: A survey. *Annual Reviews in Control*, 48, 129–146.

Nigam, N. (2014). The multiple unmanned air vehicle persistent surveillance problem: A review. *Machines*, 2(1), 13–72.

Prodan, I., Olaru, S., Bencatel, R., de Sousa, J.B., Stoica, C., and Niculescu, S.I. (2013). Receding horizon flight control for trajectory tracking of autonomous aerial vehicles. *Control Engineering Practice*, 21(10), 1334–1349.

Raković, S.V. and Lazar, M. (2012). Minkowski terminal cost functions for mpc. *Automatica*, 48(10), 2721–2725.

Sarunic, P. and Evans, R. (2014). Hierarchical model predictive control of uavs performing multitarget-multisensor tracking. *IEEE Transactions on Aerospace and Electronic Systems*, 50(3), 2253–2268.

Tabuada, P. (2007). Event-triggered real-time scheduling of stabilizing control tasks. *IEEE Transactions on Automatic Control*, 52(9), 1680–1685.

Wu, P.P.Y., Campbell, D., and Merz, T. (2010). Multi-objective four-dimensional vehicle motion planning in large dynamic environments. *IEEE Transactions on Systems, Man, and Cybernetics, Part B (Cybernetics)*, 41(3), 621–634.